

NANO EXPRESS

Open Access



Multicolor Emission from Ultraviolet GaN-Based Photonic Quasicrystal Nanopyramid Structure with Semipolar $\text{In}_x\text{Ga}_{1-x}\text{N}/\text{GaN}$ Multiple Quantum Wells

Cheng-Chang Chen^{1*}, Hsiang-Ting Lin^{2,3}, Shih-Pang Chang³, Hao-Chung Kuo³, Hsiao-Wen Hung¹, Kuo-Hsiang Chien¹, Yu-Choung Chang¹ and M. H. Shih^{2,3*}

Abstract

In this study, we demonstrated large-area high-quality multi-color emission from the 12-fold symmetric GaN photonic quasicrystal nanorod device which was fabricated using the nanoimprint lithography technology and multiple quantum wells regrowth procedure. High-efficiency blue and green color emission wavelengths of 460 and 520 nm from the regrown $\text{In}_x\text{Ga}_{1-x}\text{N}/\text{GaN}$ multiple quantum wells were observed under optical pumping conditions. To confirm the strong coupling between the quantum well emissions and the photonic crystal band-edge resonant modes, the finite-element method was applied to perform a simulation of the 12-fold symmetry photonic quasicrystal lattices.

Keywords: GaN, GaN-based LEDs, Photonic quasicrystal multicolor emission, Finite-element method

Background

The GaN-based materials with the wide band gap and unique properties had been applied in many optoelectronic systems and devices, including light emitting diodes (LEDs) [1–3] and laser diodes (LDs) [4, 5]. The GaN-based LEDs have been applied in traffic signals, display backlights [6–8], solid-state lighting [9, 10], biosensors [11], and optogenetics [12]. One of the challenges for the advanced GaN LEDs is to realize the phosphor-free white LEDs, including multichip white LEDs, monolithic LEDs, and color-conversion white LEDs [13, 14]. GaN-based nanorod LED with low dislocation, low internal field, and high light extraction efficiency [15, 16] could be a possible solution. Various approaches have been

employed to increase the light extraction efficiency for III-nitride LEDs, such as rough surfaces [17–20], sapphire microlenses [21], oblique mesa structure [22], nanopyramids [23], graded refractive index materials [24], self-assembled lithography patterning [25], colloidal-based microlens arrays [26, 27], and photonic crystals [28–31]. Photonic crystals have been reported in quasicrystal or defective two-dimensional (2D) grating configurations and lead to improved light extraction efficiency in LEDs [32–35]. The photonic crystal structure is periodic with translational symmetry. The periodic structure can exhibit a photonic band gap to inhibit the propagation of guided modes and uses a photonic crystal structure to couple guided modes with radiative modes [36–39]. Photonic crystal lasers based on the band-edge effect have several advantages, such as high-power emissions, single mode operation, and coherent oscillation [40–42]. E-beam lithography and laser interference lithography have been used to produce the photonic crystal structure [43, 44]. Furthermore, because the emitting units are separated and the emission surfaces face each other, the

*Correspondence: chencc@itri.org.tw; mhshih@gate.sinica.edu.tw

¹ Energy and Environment Research Laboratories, Industrial Technology Research Institute, Hsinchu 31040, Taiwan

² Research Center for Applied Sciences (RCAS), Academia Sinica, Taipei 11529, Taiwan

Full list of author information is available at the end of the article

light can be mixed effectively. Thus, nanorods are considered to have a great advantage for improving the luminous efficiency in the green-to-red emission region, and numerous efforts have been adopted [45, 46].

However, nanoimprint lithography (NIL) offers high-level resolution, low-cost, and high throughput compared with other forms of lithography including laser interference and e-beam lithography [47–49]. In this study, we demonstrated the multiple color emission from a GaN-based 2D photonic quasicrystal (PQC)

structure as illustrated in Fig. 1. The PQC structure was fabricated using NIL [41, 42]. The total area of the PQC pattern is approximately $4\text{ cm} \times 4\text{ cm}$ (2-in. sapphire substrate) and possessed 12-fold symmetry [50, 51], with a lattice constant of approximately 750 nm, a diameter of 300 nm, and the depth of the nanopillars is approximately $1\text{ }\mu\text{m}$. The PQC structure formed a complete band gap with the regrowth of 430-nm-tall GaN pyramids and 10-pair semipolar $\{10\text{-}11\}$ $\text{In}_x\text{Ga}_{1-x}\text{N}/\text{GaN}$

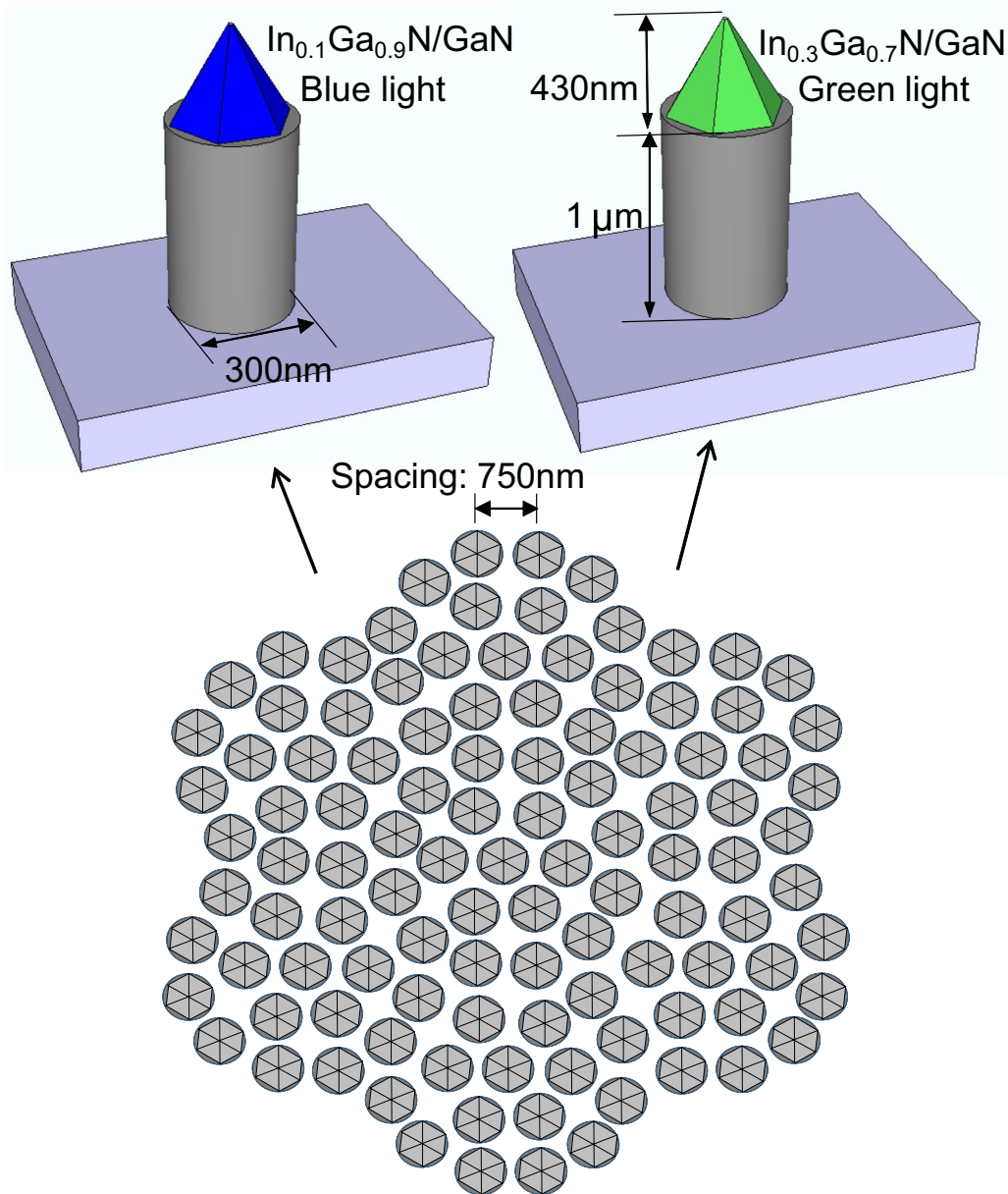


Fig. 1 Schematic structure of GaN-based PQC structure with the regrowth of semipolar $\{10\text{-}11\}$ GaN pyramids and 10-pair $\text{In}_x\text{Ga}_{1-x}\text{N}/\text{GaN}$ (3 nm/12 nm) MQW

GaN (3 nm/12 nm) multiple quantum well (MQW) nanostructures, as illustrated in Fig. 1.

Under room temperature pumping operation, the device demonstrates laser action with a low threshold power density and the multiple color emission simultaneously. We had reported the single-color laser action from the GaN PQC structure [41, 42]. This PQC platform exhibits the advantages in low fabrication costs, and better integration of GaN-based material with multi-color systems. In the future, the multiple-color GaN-based lasers can be expected with the optimization of regrowth procedure and the high-quality photonic crystal cavity.

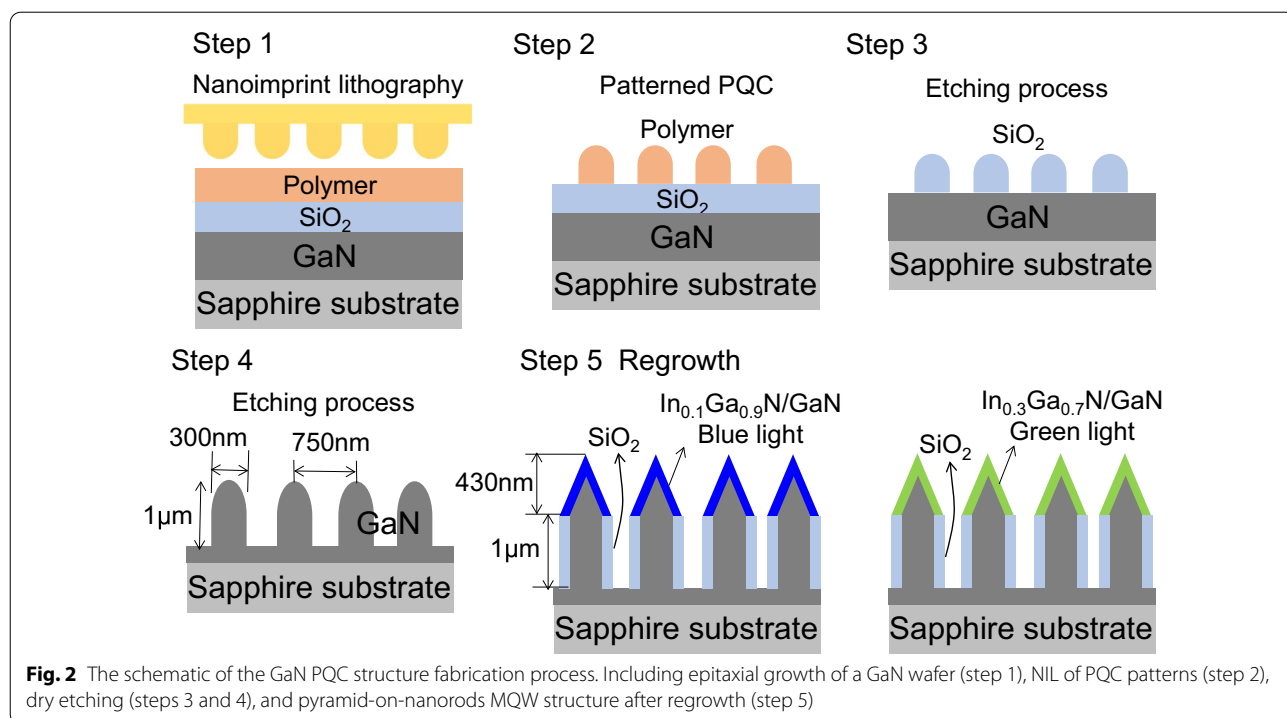
Methods

Design and Fabrication of Sample

Figure 2 illustrates the schematic procedures of the device fabrication. The fabrication procedures included epitaxial growth of a GaN wafer, NIL of PQC patterns, and dry etching. The GaN-based material was grown in a low-pressure metalorganic chemical vapor deposition reactor on a C-plane (0001) sapphire substrate. To prepare a clean surface of the sapphire substrate, the substrate was immersed into a burning solution of sulfuric acid: phosphoric acid=3:1, then heat the beaker to a constant temperature for 1 h. The substrate was cleaned with DI water under ultrasonic oscillation. A GaN (1- μm thick) was first grown on a 2-inch sapphire substrate at 1160 °C. A 0.4- μm SiO₂ mask and 0.2- μm polymer mask were then deposited. After the polymer film was dry, a

patterned mold of a 2-inch PQC structure was placed onto it by applying high pressure (Fig. 2. step 1). The substrate was heated to higher than the polymer's glass transition temperature (T_g). The substrate and the mold were then cooled to room temperature to release the mold. The PQC patterns were defined on the polymer layer (Fig. 2, step 2). The patterns were then transferred into a SiO₂ layer with reactive ion etching (RIE) by using a CHF₃/O₂ mixture (Figure, step 3). The SiO₂ layer was used as a hard mask. The structure was then etched using inductively coupled plasma RIE with a Cl₂/Ar mixture. The mask of SiO₂ layer was removed at the end of the etching process (Fig. 2, step 4).

Before the regrowth process, the sample was passivated with porous SiO₂ at the sidewall of the nanopillars. The pyramid-shaped GaN structures were regrown on top of the GaN nanopillars at 730 °C. The 0.43- μm -high pyramids contained 10-pair In_xGa_{1-x}N/GaN (3 nm/12 nm) quantum wells, which supported different wavelengths of blue and green color emission, with the ratio of in composition: In_xGa_{1-x}N/GaN-dependent InN fraction variations. In_{0.1}Ga_{0.9}N/GaN MQWs and In_{0.3}Ga_{0.7}N/GaN MQWs corresponded to 460- and 520-nm emission wavelengths, respectively (Fig. 2, step 5). The etch depth of the nanorods was approximately 1 μm , as illustrated in Fig. 3a. Figure 3b, c shows the SEM images of the PQC structure with the porous SiO₂ layer and a semipolar {10-11} In_xGa_{1-x}N/GaN MQW. Figure 3d displays the magnification of semipolar {10-11} In_xGa_{1-x}N/GaN



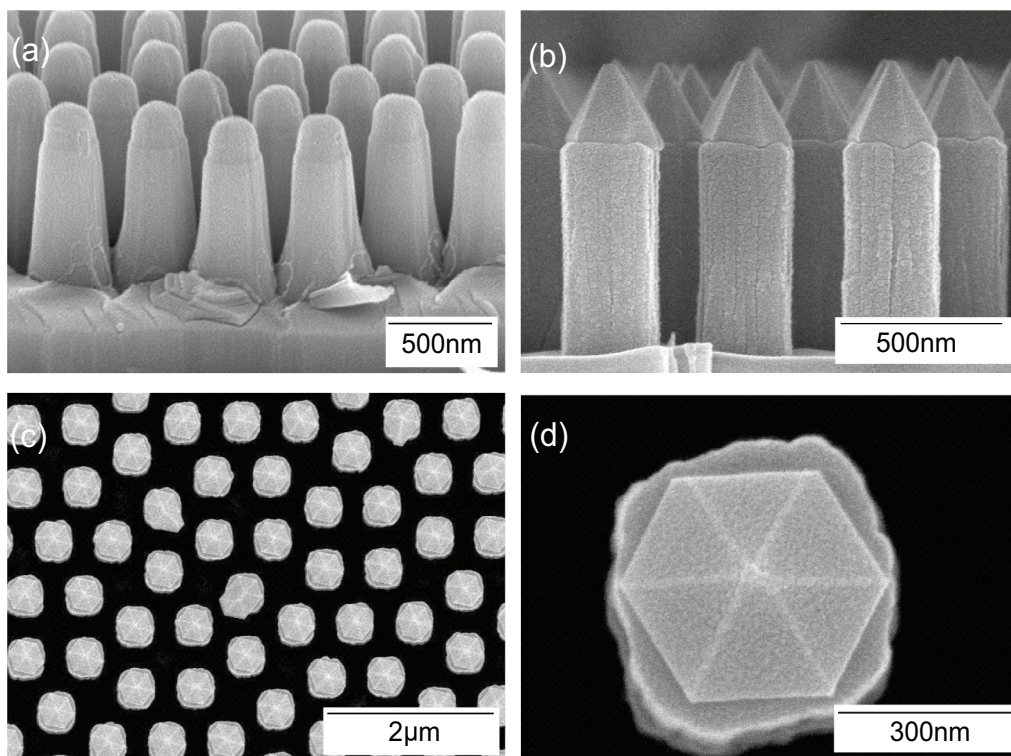


Fig. 3 **a** The tiled angle-view SEM image of the PQC structure. **b** The cross-sectional-view SEM image of the PQC structure with porous SiO_2 . **c** Top-view SEM image of the PQC structure after the regrowth procedure. **d** Magnifying SEM image of semipolar $\{10\text{-}11\}$ $\text{In}_x\text{Ga}_{1-x}\text{N}/\text{GaN}$ MQW with the facets of trapezoid microstructures

MQW with the facets of trapezoid microstructures. The semipolar $\{10\text{-}11\}$ planes can reduce the influence of the quantum-confined Stark effect on the quantum efficiency of LEDs due to the surface stability and suppression of polarization effects [52–55].

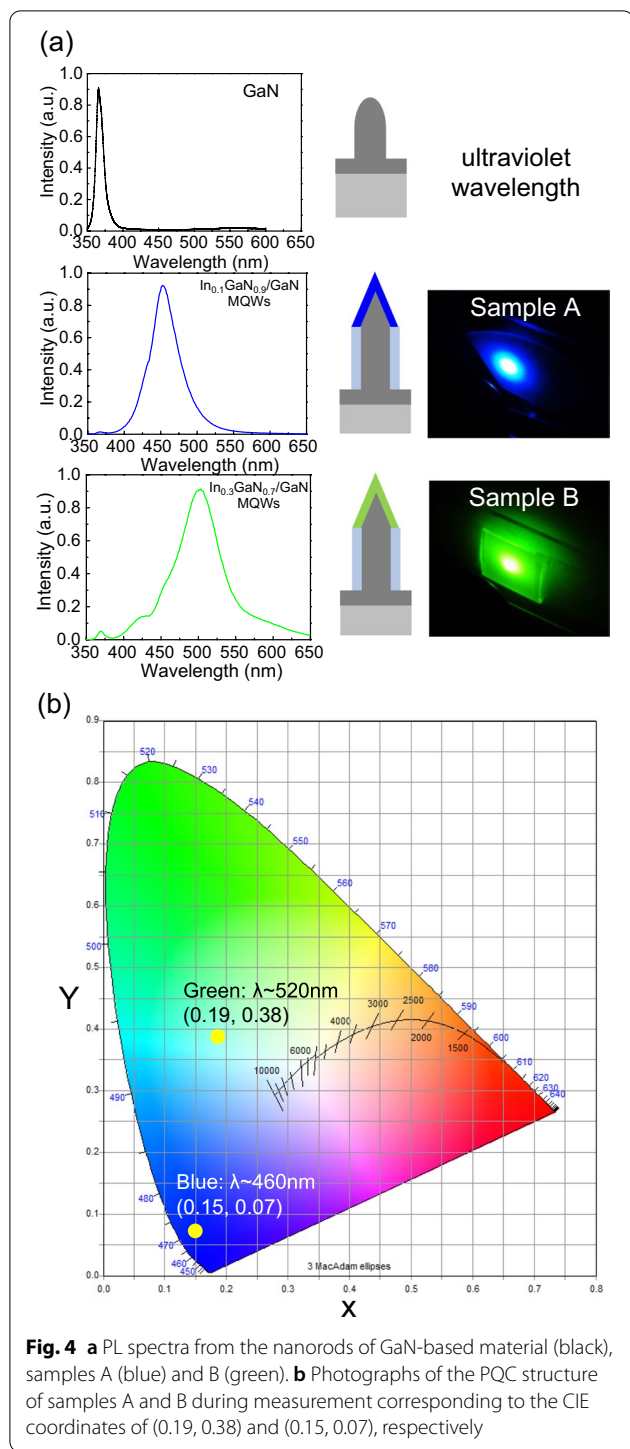
To study the optical properties of the GaN-based PQC with nanopyramid structure, two GaN PQC samples were prepared: A, $\text{In}_{0.1}\text{Ga}_{0.9}\text{N}/\text{GaN}$ MQWs, and B, $\text{In}_{0.3}\text{Ga}_{0.7}\text{N}/\text{GaN}$ MQWs with regrowth fabrication. During the regrowth step, the temperature is the key to control the ratio of indium composition. The control temperature of blue $\text{In}_{0.1}\text{Ga}_{0.9}\text{N}$ is 760–780 °C, and the control temperature of green $\text{In}_{0.3}\text{Ga}_{0.7}\text{N}$ is 730–740 °C.

Results and Discussion

To demonstrate the optical mode from the photonic quasicrystal structure, samples A and B were optically pumped by a continuous-wave (CW) He-Cd laser at 325 nm with an incident power of approximately 50 mW. The light emission from the device was collected by a $15\times$ objective lens through a multimode fiber, and coupled into a spectrometer with charge-coupled device detectors. Figure 4a illustrates the measured PL spectra under He-Cd 325 nm CW laser pumping. The spectrum

of the black curve is the light emission with a wavelength of 366 nm from the GaN-based PQC structure displayed in Fig. 3a. Both samples A (blue curve) and B (green curve) had a strong emission peak which corresponded to wavelengths of approximately 460 and 520 nm, respectively, resulting from the $\text{In}_x\text{Ga}_{1-x}\text{N}/\text{GaN}$ MQWs structure. The spectrum linewidths of the samples A and B were 40 and 60 nm, respectively. Figure 4a also displays photographs of the PQC structure of samples A and B during measurement. The CIE coordinates of PL from samples A and B were (0.19, 0.38) and (0.15, 0.07), respectively, as illustrated in Fig. 4b. Thus, this hybrid platform has several possibilities for multicolor LEDs. It should be noted that the peak of the sample B is broader than the one of sample A in Fig. 4a. The slight broad spectrum from the sample B was attributed to the existence of defects and dislocations generated by the higher indium composition [56–58].

In order to confirm the optical resonant modes were the PQC band-edge modes, the finite-element method (FEM) [59, 60] was used to perform a simulation for the 12-fold symmetry photonic quasicrystal lattices. The calculated transmission spectra of the PQC with incident angles along with 0°, 5°, 10°, 15°, 20°, and 25° as indicated

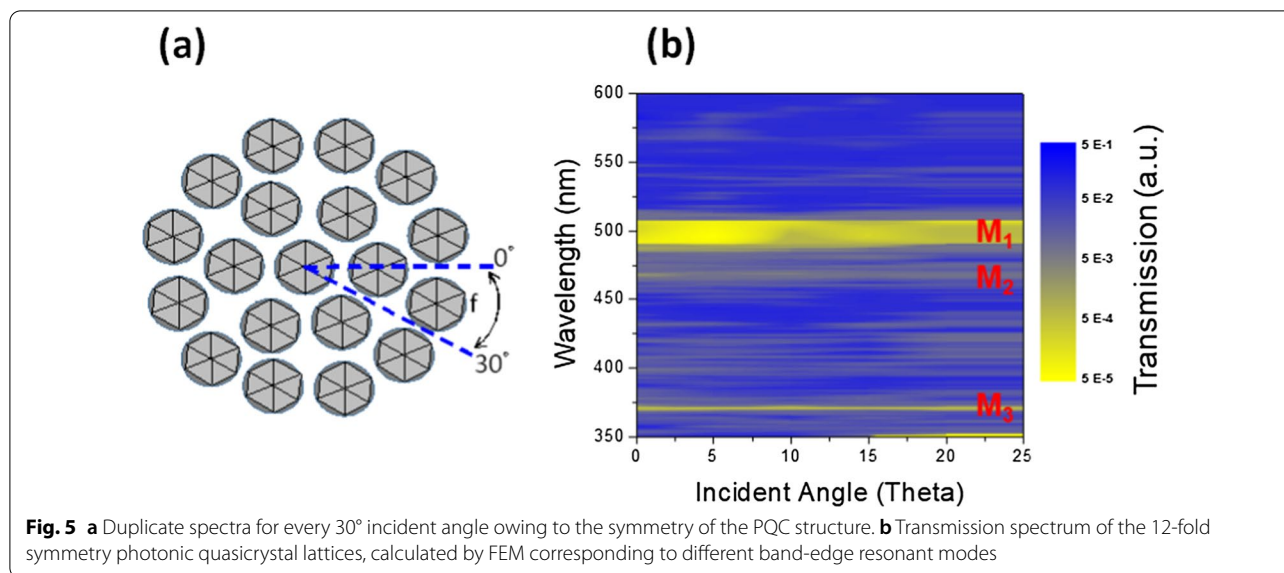


in Fig. 5a are presented in Fig. 5b. Due to the symmetry of this PQC lattices, the spectra would repeat for every 30° incident angle. The high transmission value in the spectra (blue color) indicates that the incident signal coupled into the PQC lattice resonant modes which are the band diagram areas. The low transmission (yellow color) regions

indicate several photonic band gaps (PBGs) of the PQC structure. The ratio of high-to-low transmission is more than four order which show the PQC lattices take the strong effect to select the propagation modes in the device. The observed lasing actions occur around the band-edges of the PQC bandstructure, which are the boundaries between the high-transmission and low-transmission regimes in Fig. 5b. The flat dispersion curve near the band-edge implies a low group velocity of light and strong localization and lead to the lasing actions of the devices. These PBGs matched the emission wavelength of $\text{In}_x\text{Ga}_{1-x}\text{N}/\text{GaN}$ with the corresponded normalized frequency are $a/\lambda \approx 0.88, 1.0, \text{ and } 1.25$ which were labeled as mode $M_1, M_2, \text{ and } M_3$. With the coupling between the PQC band-edge resonances and the emission from the InGaN/GaN layers, the emission efficiency and the light extraction at the specific wavelength would be further improved. The lasing action from GaN coupled to the high-frequency M_3 could be achieved under sufficient excitation as our previous demonstration [43, 45]. For the regrown $\text{In}_{0.1}\text{Ga}_{0.9}\text{N}$ and $\text{In}_{0.3}\text{Ga}_{0.7}\text{N}$ which coupled to M_2 and M_1 , the emission blue and green light would be boosted. Therefore, leveraging the coupling between the optical modes of PQC structure and $\text{In}_x\text{Ga}_{1-x}\text{N}/\text{GaN}$, efficient multicolor LEDs, LDs could be realized in such hybrid platform. The length of the nanorods in photonic crystal lattices is also important to generate the high-quality color enhancement. In this study, in order to achieve high-quality color enhancement, the photonic crystal nanorod length was etched to 1000 nm which is more than four times of the effective wavelength. To realize the multicolor emission from a single PQC device in the future, the multiple regrowth procedures should be added in the epitaxial process.

Conclusions

In summary, a 12-fold symmetric GaN PQC nanopillars was fabricated using the NIL technology. High-efficiency blue and green color emissions from $\text{In}_x\text{Ga}_{1-x}\text{N}/\text{GaN}$ MQWs were achieved with the regrowth procedure of the top $\text{In}_x\text{Ga}_{1-x}\text{N}/\text{GaN}$ MQWs grown on these facets, with an In composition ratio: $\text{In}_x\text{Ga}_{1-x}\text{N}/\text{GaN}$ -dependent InN fraction variations. The emission peaks were observed around 366-, 460-, and 520-nm wavelength resulting from $\text{In}_{0.1}\text{Ga}_{0.9}\text{N}/\text{GaN}$ MQWs and $\text{In}_{0.3}\text{Ga}_{0.7}\text{N}/\text{GaN}$ MQWs, respectively. These emission modes correspond to the band-edge resonant modes of the GaN PQC structure with FEM simulation. The methods of fabrication demonstrated a great potential to be a low-cost technique for fabricating semipolar {10-11} $\text{In}_x\text{Ga}_{1-x}\text{N}/\text{GaN}$ LED to use in manufacturing multicolor light sources. We believe that GaN-based photonic quasicrystal lasers could be integrated into multicolor light source systems in the future.



Acknowledgements

The authors are grateful to National Chiao Tung University's Center for Nano Science and Technology, the financial support from the Bureau of Energy, Ministry of Economic Affairs and the Ministry of Science and Technology (MOST), Taiwan under Grant Nos. 108-2112-M-001-044-MY2 and MOST 110-2112-M-001-053.

Authors' contributions

CCC fabricated the device, measured the optical properties and wrote the manuscript. HTL performed the modeling for photonic crystals. SPC, HWH, KHC and YCC fabricated the devices. MHS and HCK designed the devices, supervised the study and wrote the manuscript. All authors read and approved the final manuscript.

Funding

The funding and support was from the Bureau of Energy, Ministry of Economic Affairs, the Ministry of Science and Technology (MOST), Taiwan and Academia Sinica, Taiwan.

Availability of data and materials

All data supporting the conclusions of this article are included in the article.

Declarations

Competing interests

The authors declare that they have no competing interests.

Author details

¹Energy and Environment Research Laboratories, Industrial Technology Research Institute, Hsinchu 31040, Taiwan. ²Research Center for Applied Sciences (RCAS), Academia Sinica, Taipei 11529, Taiwan. ³Department of Photonics and Institute of Electro-Optical Engineering, National Chiao Tung University, Hsinchu 30010, Taiwan.

Received: 16 April 2020 Accepted: 21 July 2021

Published online: 16 September 2021

References

- Nakamura S, Mukai T, Senoh M (1994) Candela-class high-brightness InGaN/AlGaIn double-heterostructure blue-light-emitting diodes. *Appl Phys Lett* 64:1687–1689
- Nakamura S, Senoh M, Iwasa N, Nagahama S (1995) High-brightness InGaN blue, green and yellow light-emitting diodes with quantum well structures. *Jpn J Appl Phys* 34:L797–L799
- Nakamura S, Senoh M, Nagahama SI, Iwasa N, Yamada T, Matsushita T, Sugimoto Y, Kiyoku H (1997) Room-temperature continuous-wave operation of InGaIn multi-quantum-well-structure laser diodes with a long lifetime. *Appl Phys Lett* 70:868–870
- Nakamura S (1998) The roles of structural imperfections in InGaIn-based blue light-emitting diodes and laser diodes. *Science* 281:956–961
- Haberer ED, Sharma R, Meier C, Stonas AR, Nakamura S, DenBaars SP, Hu EL (2004) Free-standing, optically pumped, GaN/InGaInGaN/InGaIn microdisk lasers fabricated by photoelectrochemical etching. *Appl Phys Lett* 85:5179–5181
- Forrest SR (2004) The path to ubiquitous and low-cost organic electronic appliances on plastic. *Nature* 428:911–918
- Tsao JY (2004) Solid-state lighting: lamps, chips, and materials for tomorrow. *IEEE Circuits Devices Mag* 20:28–37
- Kim TH, Cho KS, Lee EK, Lee SJ, Chae J, Kim JW, Kim DH, Kwon JY, Amarantunga G, Lee SY, Choi BL, Kuk Y, Kim JM, Kim K (2011) Full-colour quantum dot displays fabricated by transfer printing. *Nature Photon* 5(3):176–182
- Nakamura S (1997) III–V nitride based light-emitting devices. *Solid State Commun* 102:237–248
- Shen Z, Burrows PE, Bulovic V, Forrest SR, Thompson ME (1997) Three-color, tunable, organic light-emitting devices. *Science* 276:2009–2011
- Xu H, Zhang J, Davitt KM, Song YK, Nurmikko AV (2008) Application of blue–green and ultraviolet micro-LEDs to biological imaging and detection. *J Phys D Appl Phys* 41:094013-1-13
- Wu F, Stark E, Ku PC, Wise KD, Buzsáki G, Yoon E (2015) Monolithically integrated LEDs on silicon neural probes for high-resolution optogenetic studies in behaving animals. *Neuron* 88:1136–1138
- Zhuang Z, Guo X, Liu B, Hu F, Li Y, Tao T, Dai J, Zhi T, Xie Z, Chen P, Chen D, Ge H, Wang X, Xiao M, Shi Y, Zheng Y, Zhang R (2016) High color rendering index hybrid III-nitride/nanocrystals white light-emitting diodes. *Adv Funct Mater* 26:36–43
- Feng LS, Liu Z, Zhang N, Xue B, Wang JX, Li JM (2019) Effect of nanorod diameters on optical properties of GaN-based dual-color nanorod arrays. *Chinese Phys Lett* 36: 027802-1-4
- Sekiguchi H, Kishino K, Kikuchi A (2010) Emission color control from blue to red with nanocolumn diameter of InGaIn/GaN nanocolumn arrays grown on same substrate. *Appl Phys Lett* 96:231104-1-3
- Li S, Wang X, Fündling S, Erenburg M, Ledig J, Wei J, Wehmann HH, Waag A, Bergbauer W, Mandl M, Strassburg M, Trampert A, Jahn U, Riechert H, Jönen H, Hangleiter A (2012) Nitrogen-polar core-shell GaN

- light-emitting diodes grown by selective area metalorganic vapor phase epitaxy. *Appl Phys Lett* 101:032103-1-4
17. Huh C, Lee KS, Kang EJ, Park SJ (2003) Improved light-output and electrical performance of InGaN-based light-emitting diode by microroughening of the p-GaN surface. *J Appl Phys* 93:9383–9385
 18. Fujii T, Gao Y, Sharma R, Hu EL, DenBaars SP, Nakamura S (2004) Increase in the extraction efficiency of GaN-based light-emitting diodes via surface roughening. *Appl Phys Lett* 84:855–857
 19. Lin CF, Yang ZJ, Zheng JH, Dai JJ (2005) Enhanced light output in nitride-based light-emitting diodes by roughening the mesa sidewall. *IEEE Photon Technol Lett* 17:2038–2040
 20. Huang HW, Chu JT, Kao CC, Hseuh TH, Lu TC, Kuo HC, Wang SC, Yu CC (2005) Enhanced light output of an InGaN/GaN light emitting diode with a nano-roughened p-GaN surface. *Nanotechnology* 16:1844–1848
 21. Choi HW, Liu C, Gu E, McConnell G, Girkin JM, Watson IM, Dawson MD (2004) GaN micro-light-emitting diode arrays with monolithically integrated sapphire microlenses. *Appl Phys Lett* 84:2253–2255
 22. Lee JS, Lee J, Kim S, Jeon H (2007) Fabrication of reflective GaN mesa sidewalls for the application to high extraction efficiency LEDs. *Phys Stat Sol (c)* 4:2625–2628
 23. Xi JQ, Luo H, Pasquale AJ, Kim JK, Schubert EF (2006) Enhanced light extraction in GaInN light-emitting diode with pyramid reflector. *IEEE Photon Technol Lett* 18:2347–2349
 24. Xi JQ, Schubert MF, Kim JK, Schubert EF, Chen M, Lin SY, Liu W, Smart JA (2007) Optical thin-film materials with low refractive index for broadband elimination of Fresnel reflection. *Nature Photon* 1:176–179
 25. Chhajed S, Lee W, Cho J, Schubert EF, Kim JK (2011) Strong light extraction enhancement in GaInN light-emitting diodes by using self-organized nanoscale patterning of pp-type GaN. *Appl Phys Lett* 98:071102-1-3
 26. Li XH, Song R, Ee YK, Kumnorkaew P, Gilchrist JF, Tansu N (2011) Light extraction efficiency and radiation patterns of III-nitride light-emitting diodes with colloidal microlens arrays with various aspect ratios. *IEEE Photonics J* 3:489–499
 27. Ee YK, Arif RA, Tansu N, Kumnorkaew P, Gilchrist JF (2007) Enhancement of light extraction efficiency of InGaN quantum wells light emitting diodes using SiO₂/polystyrene microlens arrays. *Appl Phys Lett* 91:201107-1-3
 28. Kim DH, Cho CO, Roh YG, Jeon H, Park YS, Cho J, Im JS, Sone C, Park Y, Choi WJ, Park QH (2005) Enhanced light extraction from GaN-based light-emitting diodes with holographically generated two-dimensional photonic crystal patterns. *Appl Phys Lett* 87:203508-1-3
 29. Kim T, Danner AJ, Choquette KD (2005) Enhancement in external quantum efficiency of blue light-emitting diode by photonic crystal surface grating. *Electron Lett* 41:1138–1139
 30. Wierer JJ, David A, Megens MM (2009) III-nitride photonic-crystal light-emitting diodes with high extraction efficiency. *Nat Photon* 3:163–169
 31. Rangel E, Matioli E, Choi YS, Weisbuch C, Speck JS, Hu EL (2011) Directionality control through selective excitation of low-order guided modes in thin-film InGaN photonic crystal light-emitting diodes. *Appl Phys Lett* 98:081104-1-3
 32. Shakya J, Kim KH, Lin JY, Jiang HX (2004) Enhanced light extraction in III-nitride ultraviolet photonic crystal light-emitting diodes. *Appl Phys Lett* 85:142–144
 33. Wierer JJ, Krames MR, Epler JE, Gardner NF, Craford MG, Wendt JR, Simmons JA, Sigalas MM (2004) InGaN/GaN quantum-well heterostructure light-emitting diodes employing photonic crystal structures. *Appl Phys Lett* 84:3885–3887
 34. Matioli E, Rangel E, Iza M, Fleury B, Pfaff N, Speck J, Hu E, Weisbuch C (2010) High extraction efficiency light-emitting diodes based on embedded air-gap photonic-crystals. *Appl Phys Lett* 96:031108-1-3
 35. Jewell J, Simeonov D, Huan SC, Hu YL, Nakamura S, Speck J, Weisbuch C (2012) Double embedded photonic crystals for extraction of guided light in light-emitting diodes. *Appl Phys Lett* 100:171105-1-4
 36. Boroditsky M, Krauss TF, Coccioli R, Vrijen R, Bhat R, Yablonoitch E (1999) Light extraction from optically pumped light-emitting diode by thin-slab photonic crystals. *Appl Phys Lett* 75:1036–1038
 37. Rattier M, Benisty H, Schwoob E, Weisbuch C, Krauss TF, Smith CJM, Houdré R, Oesterle U (2003) Omnidirectional and compact guided light extraction from Archimedean photonic lattices. *Appl Phys Lett* 83:1283–1285
 38. Delbeke D, Bienstman P, Bockstaele R, Baets R (2002) Rigorous electromagnetic analysis of dipole emission in periodically corrugated layers: the grating-assisted resonant-cavity light-emitting diode. *J Opt Soc Am A* 19:871–880
 39. David A, Fujii T, Sharma R, McGroddy K, Nakamura S, DenBaars SP, Hu EL, Weisbuch C, Benisty H (2006) Photonic-crystal GaN light-emitting diodes with tailored guided modes distribution. *Appl Phys Lett* 88:061124-1-3
 40. Matsubara H, Yoshimoto S, Saito H, Jianglin Y, Tanaka Y, Noda S (2008) GaN photonic-crystal surface-emitting laser at blue-violet wavelengths. *Science* 319:445–447
 41. Chen CC, Chiu CH, Tu PM, Kuo MY, Shih MH, Huang JK, Kuo HC, Zan HW, Chang CY (2012) Large area of ultraviolet GaN-based photonic quasicrystal laser. *Jpn J Appl Phys* 51:04DG02-1-3
 42. Chen CC, Chiu CH, Chang SP, Shih MH, Kuo MY, Huang JK, Kuo HC, Chen SP, Lee LL, Jeng MS (2013) Large-area ultraviolet GaN-based photonic quasicrystal laser with high-efficiency green color emission of semipolar {10-11} In_{0.3}Ga_{0.7}N/GaN multiple quantum wells. *Appl Phys Lett* 102:011134-1-4
 43. Yu H, Yu J, Sun F, Li Z, Chen S (2007) Systematic considerations for the patterning of photonic crystal devices by electron beam lithography. *Opt Commun* 271:241–247
 44. Vogelaar L, Nijdam W (2001) Large area photonic crystal slabs for visible light with waveguiding defect structures: fabrication with focused ion beam assisted laser interference lithography. *Adv Mater* 13:1551–1554
 45. Nguyen HPT, Cui K, Zhang S, Djavid M, Korinek A, Botton GA, Mi Z (2012) Controlling electron overflow in phosphor-free InGaN/GaN nanowire white light-emitting diodes. *Nano Lett* 12:1317–1323
 46. Li W, Li K, Kong FM, Yue QY, Chen XL, Yu XJ (2014) Study of light extraction efficiency of GaN-based light emitting diodes by using top micro/nanorod hybrid arrays. *Opt Quant Electron* 46:1413–1423
 47. Farrell RM, Young EC, Wu F, DenBaars SP, Speck JS (2012) Materials and growth issues for high-performance nonpolar and semipolar light-emitting devices. *Semicond Sci Technol* 27:024001-1-14
 48. Browne DA, Young EC, Lang JR, Hurni CA, Speck JS (2012) Indium and impurity incorporation in InGaN films on polar, nonpolar, and semipolar GaN orientations grown by ammonia molecular beam epitaxy. *J Vac Sci Tech A* 30:041513–041520
 49. Zhao H, Liu G, Zhang J, Poplawsky JD, Dierolf V, Tansu N (2011) Approaches for high internal quantum efficiency green InGaN light-emitting diodes with large overlap quantum wells. *Opt Express* 19:A991–A1007
 50. Huang HW, Lin CH, Lee KY, Yu CC, Huang JK, Lee BD, Kuo HC, Leung KM, Wang SC (2009) Enhanced light output power of GaN-based vertical-injection light-emitting diodes with a 12-fold photonic quasi-crystal by nano-imprint lithography. *Semicond Sci Technol* 24:085008-1-5
 51. Zoorob ME, Charlton MDB, Parker GJ, Baumberg JJ, Netti MC (2000) Complete photonic bandgaps in 12-fold symmetric quasicrystals. *Nature* 404:740–743
 52. Nishizuka K, Funato M, Kawakami Y, Fujita SG, Narukawa Y, Mukai T (2004) Efficient radiative recombination from (11̄2̄2)X(112̄2̄)-oriented In_xGa_{1-x}NIn_yGa_{1-y}N multiple quantum wells fabricated by the regrowth technique. *Appl Phys Lett* 85:3122–3124
 53. Neubert B, Brückner P, Habel F, Scholz F, Riemann T, Christen J, Beer M, Zweck J (2005) GaInN quantum wells grown on facets of selectively grown GaN stripes. *Appl Phys Lett* 87:182111-1–182113
 54. Haller C, Carlin JF, Jacopin G, Martin D, Butté R, Grandjean N (2017) Burying non-radiative defects in InGaN underlayer to increase InGaN/GaN quantum well efficiency. *Appl Phys Lett* 111: 262101-1-5
 55. Tangi M, Mishra P, Janjua B, Prbaswara A, Zhao C, Priante D, Min JW, Ng TK, Ooi BS (2018) Role of quantum-confined stark effect on bias dependent photoluminescence of N-polar GaN/InGaN multi-quantum disk amber light emitting diodes. *J Appl Phys* 123:105702-1-8
 56. Puchtler TJ, Woolf A, Zhu T, Gachet D, Hu EL, Oliver RA (2014) Effect of threading dislocations on the quality factor of InGaN/GaN Microdisk Cavities. *ACS Photonics* 2:137–143
 57. Shim HW, Choi RJ, Jeong SM, Vinh LV, Hong CH, Suh EK, Lee HJ, Kim YW, Hwang YG (2002) Influence of the quantum-well shape on the light emission characteristics of InGaN/GaN quantum-well structures and light-emitting diodes. *Appl Phys Lett* 81:3552–3554
 58. Massabuau FCP, Horton MK, Pearce E, Hammersley S, Chen P, Zielinski MS, Weatherley TFK, Divitini G, Edwards PR, Kappers MJ, McAleese C, Moram MA, Humphreys CJ, Dawson P, Oliver RA (2019) Optical and structural properties of dislocations in InGaN. *J Appl Phys* 125:165701-1-10

59. Kim WJ, O'Brien JD (2004) Optimization of a two-dimensional photonic-crystal waveguide branch by simulated annealing and the finite-element method. *J Opt Soc Am B* 21:289–295
60. Andonegui I, Garcia-Adeva AJ (2013) The finite element method applied to the study of two-dimensional photonic crystals and resonant cavities. *Opt Express* 21:4072–4092

Publisher's Note

Springer Nature remains neutral with regard to jurisdictional claims in published maps and institutional affiliations.

Submit your manuscript to a SpringerOpen[®] journal and benefit from:

- ▶ Convenient online submission
- ▶ Rigorous peer review
- ▶ Open access: articles freely available online
- ▶ High visibility within the field
- ▶ Retaining the copyright to your article

Submit your next manuscript at ▶ [springeropen.com](https://www.springeropen.com)
